

A New Synthetic Route to Soluble Polyquinolines with Tunable Photophysical, Redox, and Electroluminescent Properties

Christopher J. Tonzola, Maksudul M. Alam, and Samson A. Jenekhe*

Department of Chemical Engineering and Department of Chemistry, University of Washington, Seattle, Washington 98195-1750

Received June 17, 2005; Revised Manuscript Received September 11, 2005

ABSTRACT: A new monomer bearing dialkyl groups, 3,3'-dinonanoylbenzidine, when copolymerized with diacetyl monomers gave six new alternating conjugated copolymers, poly(2,2'-arylene-4,4'-bis(4-alkylquinolines))s, which are soluble in organic solvents. The thermal, electrochemical, photophysical, and electroluminescent properties of the new polyquinolines varied with the arylene linkage, including *p*-phenylene, 4,4'-biphenylene, stilbene, 5,5'-bithienylene, bis(thienyl)vinylene, and 3,7-phenothiazinylene. The new conjugated polymers combined high glass transition temperature (110–254 °C) with quasi-reversible electrochemical reduction from which 2.72–3.00 eV electron affinities were estimated. The optical band gap varied from 2.19 to 2.86 eV whereas the photoluminescence emission maximum varied from blue-green (477 nm) to deep red (646 nm). Some of the new polymers with alternating donor–acceptor architecture showed strong intramolecular charge transfer. Electroluminescence of moderate brightness (up to 209 cd/m²) was achieved with blue-green, green, yellow, orange, and deep red colors depending on the arylene linkage of the copolymer. The new polyquinolines were also demonstrated as useful electron transport materials for the enhancement of polymer light-emitting diodes.

Introduction

New and improved conjugated polymer semiconductors are necessary for the advancement of the rapidly growing field of organic electronics.^{1–5} One area of great need is the development of new n-type conjugated polymers with good electron transport properties and a range of electron affinities or lowest unoccupied molecular orbital (LUMO) energy levels.^{1,2} For use as electron transport materials in organic light-emitting diodes (OLEDs) a desirable range of the electron affinity (EA) is 2.7–3.4 eV, whereas much higher values (EA ~ 3.8–4.5 eV) are necessary for Ohmic contacts in photovoltaic cells and field effect transistors.^{2,3d,4} Our group and others have previously shown that poly(phenylquinoline)s⁶ and poly(alkylquinoline)s⁷ are excellent electron transport materials for OLEDs due in part to their suitable EA values (2.6–3.0 eV) and rugged photochemical and thermal stability (*T*_g > 100 °C). Improved solubility, processability, and modulation of the electronic and photonic properties are of current interest in the development of polyquinolines as n-type semiconductors for organic electronics.^{6c,d,7–10}

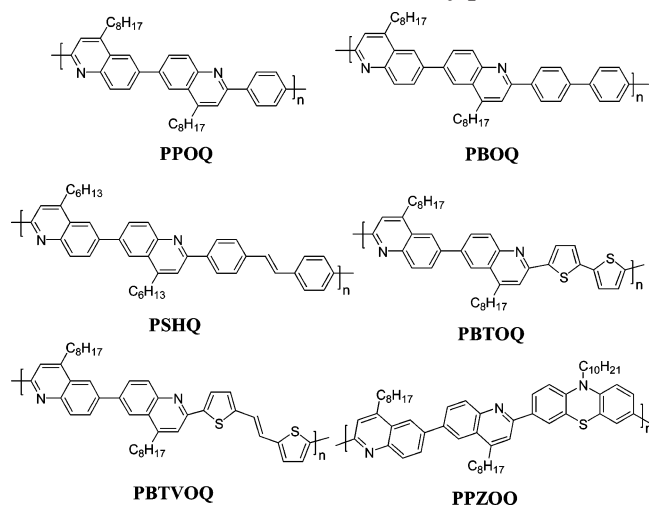
Early efforts to address the problem of processing conjugated poly(phenylquinoline)s into thin films suitable for nonlinear optics, optoelectronics, and electronics exploited their solubility in protonic acids (e.g., formic acid) and solubility of their Lewis acid complexes in aprotic organic solvents.¹¹ Processability from formic acid allowed the poly(phenylquinoline)s to be successfully used in bilayer OLED devices with emissive p-type (hole transport) polymers such as poly(*p*-phenylenevinylene) (PPV)^{6a,b} and poly(2-methoxy-5-(2'-ethyl-hexyloxy)-1,4-phenylenevinylene) (MEH–PPV).^{6c–f,7} Recent synthetic work has targeted organic-solvent-soluble polyquinolines in an effort to enhance processability and to permit more comprehensive characterization (e.g., solution spectroscopy on the neutral, nonprotonated species and gel permeation chromatography).^{6c,d,7–10}

Solubility in organic solvents also allows for the preparation of blends with other conjugated polymers—an attractive route to efficient photovoltaic and light-emitting materials where both n-type and p-type functionalities are needed.¹² Furthermore, soluble polyquinolines can be used as the host in guest–host systems with either fluorescent or phosphorescent emissive dopants as has been done with other soluble polymers.¹³ To achieve solubility in organic solvents, alkyl-substituted arylene groups^{6c,d,8b,c,9,10} have been incorporated into the polymer backbone or the pendant phenyl group on the bis(4-phenylquinoline) has been alkylated.^{8a} Alternatively, our group has synthesized a series of A–B monomers that self-polymerized into soluble regioregular poly(4-alkylquinoline)s.⁷ Although polyquinolines have been studied for over three decades, novel architectures such as diblock and triblock copolymers¹⁴ that facilitate self-assembly and side-chain polymers¹⁵ are still being explored. Similarly, the library of arylene groups being incorporated into quinoline copolymers is being expanded and becoming more exotic.^{8–10,16}

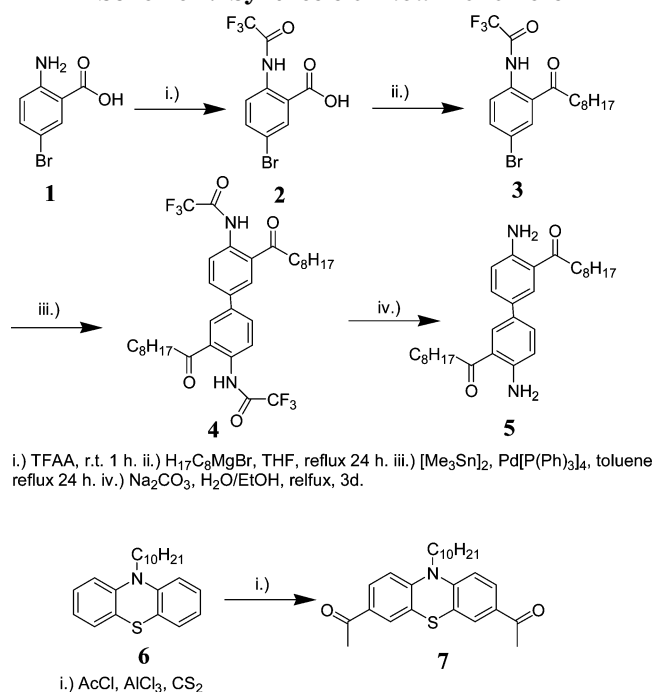
This paper reports a new synthetic route to organic-solvent-soluble conjugated polyquinolines incorporating bis(4-alkylquinoline) units through a new A–A monomer, 3,3'-dinonanoylbenzidine. A series of six new alternating conjugated copolymers, poly(2,2'-arylene-4,4'-bis(4-alkylquinoline)s), whose structures are shown in Chart 1, exemplify the new synthetic methodology. Diverse n-type conjugated polymers that are soluble in organic solvents can thus be obtained by variation of the arylene linkage which facilitates the tuning of the electronic and optical properties. The arylene linkages shown in the polymers of Chart 1 include *p*-phenylene, 4,4'-biphenylene, stilbene, 5,5'-bithienylene, bis(thienyl)vinylene, and 3,7-phenothiazinylene, and they allowed the variation of the electron affinity in the 2.7–3.0 eV range, the glass transition in the 110–254 °C range, and the electroluminescence color from blue-green, green, yellow, and orange to deep red.

* Corresponding author. E-mail: jenekhe@u.washington.edu.

Chart 1. Structures of New Polyquinolines



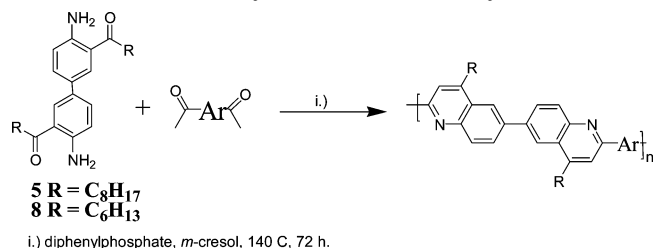
Scheme 1. Synthesis of New Monomers



Results and Discussion

Synthesis and Characterization. The syntheses of the new monomers **5** and **7** are outlined in Scheme 1. The reaction of alkylmagnesium bromide with *N*-(trifluoroacetyl)-5-bromoanthranilic acid (**2**) is the crucial step in achieving *o*-(amino keto) functionality. Attempts to synthesize the monomer via Friedel–Crafts acylation of aniline, 4-bromoaniline, and benzidine were unsuccessful. *N*-Protected-5-bromo-2-nonanoylaniline (**3**) was coupled under Stille conditions and then deprotected to achieve the 3,3'-dininanoylbis(2-aminobenzoic acid) (**5**). The overall yield of the four-step synthesis was 24%. Initial work targeted the 3,3'-diheptanoylbis(2-aminobenzoic acid) (**8**), the synthesis of which is described elsewhere.¹⁰ However, the poly(2,2'-(arylene)-6,6'-bis(4-hexylquinolines)) based on **8** had poor solubility,¹⁰ leading us to increase the length of the alkyl chain from hexyl to octyl in the present study. Diacetyl monomers were copolymerized with the (*o*-amino keto)-functionalized 3,3'-dininanoylbis(2-aminobenzoic acid) (**5**) to yield the new polyquinolines containing bis(4-octylquinoline) in the main chain (Scheme 2). 3,3'-

Scheme 2. Synthesis of New Polymers



Diheptanoylbis(2-aminobenzoic acid) (**8**) was initially used to synthesize several polymers containing bis(4-hexylquinoline); however, only PSHQ (Chart 1) was sufficiently soluble in organic solvents and incorporated in the present study. The resulting products of polymerization were precipitated into 10% triethylamine/ethanol and extracted on a Soxhlet apparatus with 20% triethylamine/ethanol for 2 days to remove the diphenyl phosphate (DPP) acid catalyst.

¹H NMR and FT-IR spectra of the polymers confirmed the proposed structures. Thermogravimetric analysis (TGA) also indicated high purity with <2% weight loss at the decomposition temperatures (*T_D*). The weight-average molecular weights (*M_w*), based on polystyrene standards and gel permeation chromatography (GPC), are shown in Table 1. The *M_w* values range from 10 000 for PPZOQ to 33 900 for PBOQ, and the polydispersities were in the range of 1.26–4.90. These *M_w* values are generally lower than those previously reported for soluble poly(phenylquinoline)s^{6c,d} but are similar to those of poly(4-alkylquinoline)s.⁷ This indicates that replacing the phenyl group with an alkyl chain at the keto position of the A–A monomer may decrease the reactivity of the monomer. The much larger and broader molecular weight of PBOQ compared to the others reflects the geometry and reactivity of diacetyl biphenyl as also observed in prior phenylated polyquinolines.¹¹

The TGA thermogram of PBOQ is shown in Figure 1, indicating a decomposition temperature of 419 °C. The decomposition temperature (*T_D*) of the remaining polymers was in the range of 400–477 °C (Table 1). Typical second heating differential scanning calorimetry (DSC) scans for PPOQ and PBOQ are shown in Figure 2; these polymers show glass transitions (*T_g*) of 127 and 141 °C, respectively. The *T_g* of the remaining polymers was between 110 and 254 °C (Table 1). Notably, the hexyl-substituted PSHQ had a significantly higher *T_g* (254 °C) than the octyl-substituted polyquinolines (*T_g* < 170 °C), and PPZOQ (*T_g* = 110 °C), which contains both a decyl chain and two octyl chains per repeat unit, has the lowest *T_g*. Poly(phenylquinoline)s typically have glass transitions between 200 and 400 °C.¹¹ The presence and length of alkyl chains has a significant effect on the glass transition as evidenced in a series of poly(phenylquinoline)s containing dialkylbithiophene moieties in the main chain;^{6c,d} it was observed that the *T_g* decreased with increasing chain length. The high glass transitions of the new polyquinolines (>110 °C) suggest that they could withstand the joule heating associated with the operation of organic electronic devices.

Electrochemical Properties. Cyclic voltammetry was performed on thin films of the polymers coated onto Pt wire. Representative cyclic voltammograms (CVs) of four of the new polyquinolines are shown in Figure 3, and the corresponding electrochemical redox data are collected in Table 2. CV scans on the polymers showed quasi-reversible reduction waves, similar to those of

Table 1. Physical Properties of New Polyquinolines

polymer	$M_w (10^4)$	PDI	T_D (°C)	T_g (°C)	$\lambda_{\max}^{\text{abs}}$ (soln) (nm)	ϵ ($10^4 \text{ M}^{-1} \text{ cm}^{-1}$)	$\lambda_{\max}^{\text{abs}}$ (film) (nm)	E_g^{opt} (eV)	$\lambda_{\max}^{\text{em}}$ (soln) (nm)	$\lambda_{\max}^{\text{em}}$ (film) (nm)	ϕ_f (soln)	ϕ_f (film)
PPOQ	1.5	1.82	421	127	375	2.3	386	2.85	417	493	.18	.05
PBOQ	3.3	4.90	419	141	372	2.4	385	2.86	413	477	.13	.06
PSHQ	1.9	2.74	477	254	398	1.4	409	2.67	431	524	.11	.04
PBTOQ	1.5	1.45	400	128	436	2.3	443	2.35	483	615	.16	.01
PBTVOQ	1.1	1.50	445	163	453	1.0	454	2.19	502	646	.20	.07
PPZOQ	1.0	1.26	414	110	414	1.5	429	2.29	538	576	.24	.08

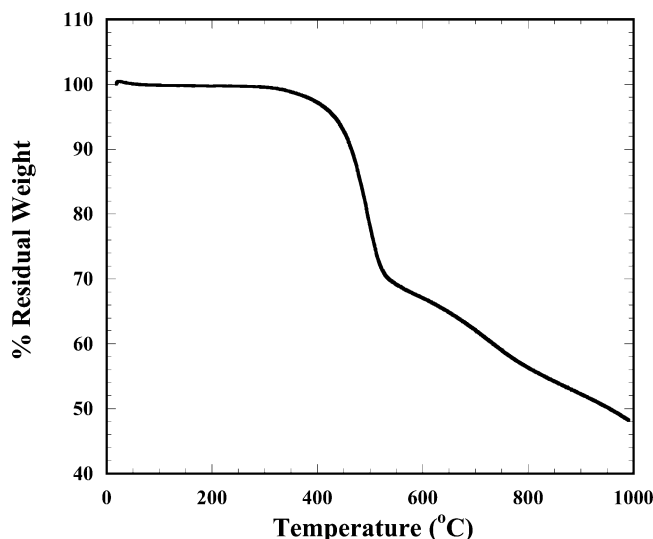


Figure 1. TGA curve of PBOQ at a scan rate of 10 °C/min.

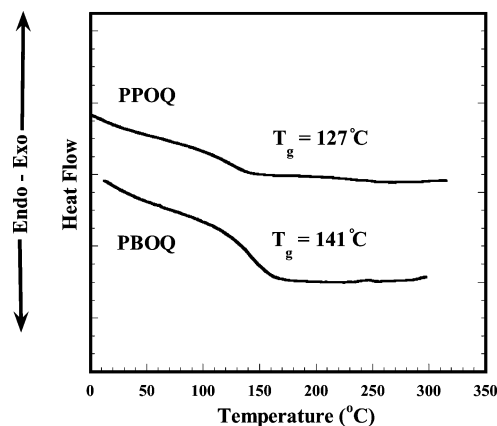


Figure 2. Second heating DSC curves of PPOQ and PBOQ (rate = 10 °C/min).

previously reported polyquinolines.^{6c,d,7,17} The formal reduction potential ($E_{\text{red}}^{\text{red}} = (E_{\text{pa}} + E_{\text{pc}})/2$) varied from -2.0 V (vs SCE) for PPZOQ (Figure 3c) to -1.56 V for PBTVOQ. The onset reduction potential followed a trend similar to that of $E_{\text{red}}^{\text{red}}$ in which PBTOQ and PBTVOQ have the most positive values. The solid-state electron affinity (EA) was estimated using the following relationship: $\text{EA} = E_{\text{red}}^{\text{onset}} + 4.4$, where $E_{\text{red}}^{\text{onset}}$ is the onset reduction potential vs SCE.^{17,18} The EA values range from 2.72 eV for PPZOQ to 3.00 eV for PBTVOQ, reflecting the modulation of the LUMO level by the arylene linkage. These values agree well with other polyquinolines which have been found to be useful n-type materials for OLEDs.^{6b,7,10}

The electron-accepting bis(quinoline) moiety is present in all the polymers (Chart 1), which explains the little variation in electron affinity. However, variation of the arylene linkage provided a modulation of the oxidative

properties of the polymers. PPOQ did not exhibit an oxidation wave in the potential range scanned in the CVs whereas PBOQ and PSHQ (Figure 3a,b) had irreversible oxidation peaks. PBTOQ (Figure 3d) and PBTVOQ, with thiophene linkages, showed a slight reversibility in their oxidation waves, similar to that observed in analogous poly(phenylquinoline)s.¹⁷ PPZOQ, with the electron-rich phenothiazine group, showed a quasi-reversible oxidation peak (Figure 3c). The solid-state ionization potential (IP), estimated as $\text{IP} = E_{\text{ox}}^{\text{onset}} + 4.4$, where $E_{\text{ox}}^{\text{onset}}$ is the onset oxidation potential vs SCE, varied from 5.17 eV for PPZOQ to 5.96 eV for PBOQ. The electrochemically derived band gap (E_g^{el}) of the new polyquinolines (Table 2) was 2.30–3.14 eV. These values, as well as the estimated HOMO/LUMO levels, showed good agreement with previously reported, structurally similar poly(phenylquinoline)s.^{17,19} This indicates that the alkyl substitution at the 4-position had negligible effect on the electronic structure of the polymers.

Photophysical Properties. Absorption spectra of the six new polyquinolines in THF solution are shown in Figure 4a. The lowest energy absorption bands of most of the polymers are from π – π^* transitions by virtue of their large molar extinction coefficients (ϵ) ($\epsilon_{\max} = (1.0\text{--}2.3) \times 10^4 \text{ M}^{-1} \text{ cm}^{-1}$). However, the lowest energy absorption bands of PBTOQ, PPZOQ, and PBTVOQ, which have a clear donor–acceptor architecture, can be interpreted in terms of intramolecular charge transfer (ICT).^{19,20} The absorption maxima ($\lambda_{\max}^{\text{abs}}$) of the polymers varies from 372 to 453 nm. The phenylene-, biphenylene-, and stilbene-linked polymers have the lowest $\lambda_{\max}^{\text{abs}}$ values (372–398 nm). The $\lambda_{\max}^{\text{abs}}$ of PPZOQ, PBTOQ, and PBTVPQ show significant red shifts relative to these polymers because the donor–acceptor architecture of the latter polymers facilitates large ICT. Donor–acceptor architectures in conjugated polymers is a well-known route to lowering the band gap of semiconducting polymers.^{11,19,20}

The thin film optical absorption spectra of the polymers are shown in Figure 4b. The solid-state absorption bands are red-shifted by 1–15 nm compared to their corresponding solution spectra. This phenomenon of increased electronic delocalization in thin films compared to solution is indicative of increased planarity of the polymer backbones in the solid state. The λ_{\max} of the polymer thin films is in the range of 385–454 nm. Optical band gaps (E_g^{opt}) determined from the absorption edge of the thin film spectra are also shown in Table 1. The E_g^{opt} values range from 2.19 to 2.86 eV, with PBTOQ (2.35 eV) and PBTVOQ (2.19 eV) having the lowest values. These band gap values are in fair agreement with those determined from cyclic voltammetry (Table 2). A comparison of the solid-state absorption spectra of the present poly(bis(4-alkylquinoline)s) to analogous poly(phenylquinoline)s shows a blue shift

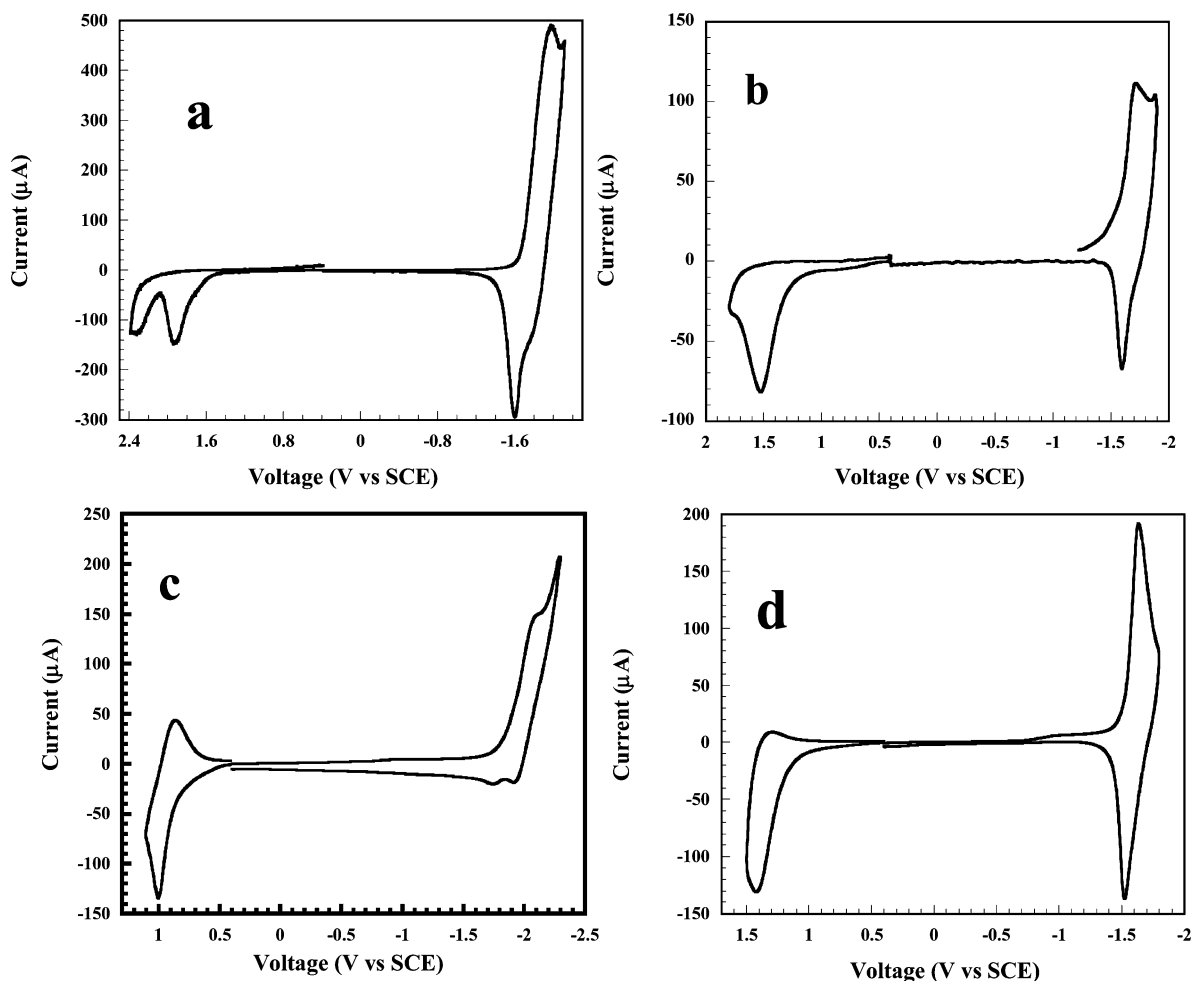


Figure 3. Cyclic voltammograms of thin films of PBOQ (a), PSHQ (b), PPZOQ (c), and PBTOQ (d) on Pt electrode. (0.1 M TBAF6 in MeCN; scan rate = 60 mV/s).

Table 2. Electrochemical Properties of New Polyquinolines^{a,b}

polymer	$E_{\text{red}}^{\text{onset}}$ (V)	$E_{\text{red}}^{\text{peak}}$ (V)	EA (eV)	$E_{\text{ox}}^{\text{peak}}$ (V)	$E_{\text{ox}}^{\text{onset}}$ (V)	IP (eV)	E_{g}^{el} (eV)
PPOQ	-1.72	-1.62	2.78	n.o.	n.o.	n.o.	n.o.
PBOQ	-1.78	-1.58	2.82	1.92	1.56	5.96	3.14
PSHQ	-1.66	-1.48	2.92	1.52	1.21	5.61	2.63
PBTOQ	-1.57	-1.42	2.98	1.43	1.03	5.43	2.45
PBTVOQ	-1.56	-1.40	3.00	1.31	0.90	5.30	2.30
PPZOQ	-2.00	-1.68	2.72	0.99	0.77	5.17	2.53

^a All potentials vs SCE. ^b Polymers were coated onto Pt wire; 0.1 M TBAPF₆/MeCN. Scan rate = 60 mV/s.

of 7–19 nm.^{11,19} This indicates that the π -orbitals of the phenyl side group have some electronic interaction with those of the backbone quinoline unit.

The dilute solution (10^{-6} M) photoluminescence (PL) spectra of the polymers in THF are shown in Figure 5a. Five of the polymers have highly structured emission bands whereas the emission band of PPZOQ is structureless. The emission maximum varies from 413 nm for PPOQ and 538 nm for PPZOQ. The PL quantum yield (ϕ_f) of the polymers in dilute solution in THF was 11–24% (Table 1). The Stokes shift is between 33 and 49 nm for the polymers, except PPZOQ in which it is 124 nm. Previously, the analogous phenothiazylene-linked poly(phenylquinoline) (PPZPQ)^{19a} was not studied in solution in the neutral state. However, the solid-state emission of PPZPQ and that of a model compound were established to be due to intramolecular excitons with strong charge-transfer character. We believe that ICT also explains the large Stokes shift in the PL emission of PPZOQ. Although the PL quantum yields

of these polymers (11–24%) are low, they are comparable to those of other soluble polyquinolines.^{6b,7,10}

The PL emission spectra of the polymer thin films are shown Figure 5b. All the PL emission spectra have broad and structureless line shapes, with emission maxima ($\lambda_{\text{max}}^{\text{em}}$) from 477 nm (PBOQ) to 646 nm (PBTVOQ). Thus, variation of the arylene linkage effectively tunes the PL emission color of the polymers. Five of the polymers showed an increased Stokes shift relative to that observed in solution. These features of the thin film PL emission spectra are indicative of aggregation effects and significant excimer formation.²¹ However, PPZOQ thin films displayed approximately the same Stokes shift as in solution, indicating that the PL emission arises from an intramolecular charge-transfer excited state. A rough estimate of the solid-state fluorescence quantum efficiencies of these films without an integrated sphere shows that they are low (1–8%), consistent with other polyquinolines.^{6c,d,7,10}

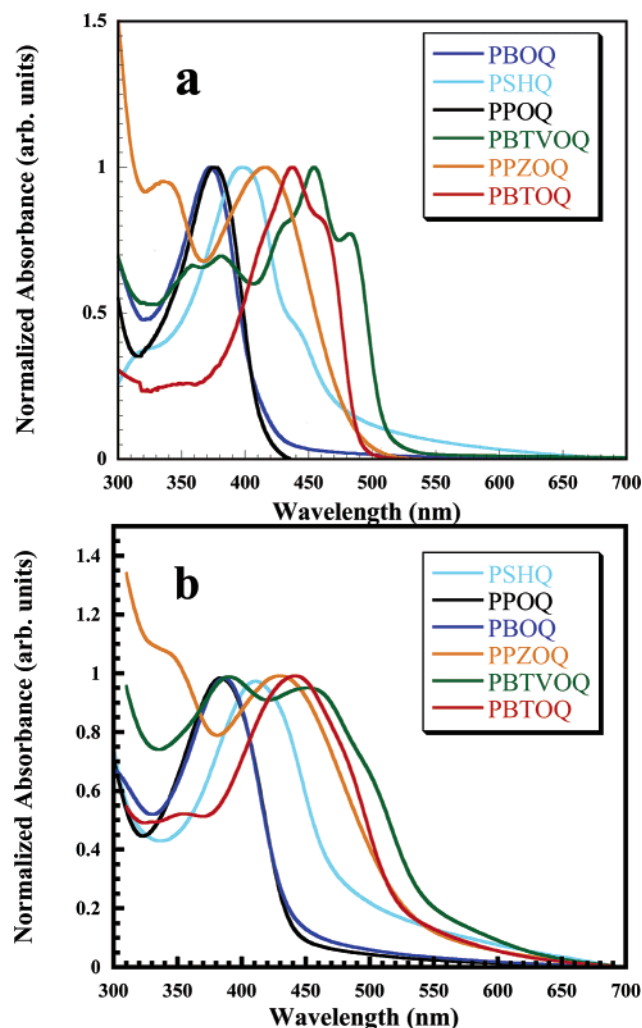


Figure 4. Optical absorption spectra of new polyquinolines in dilute THF (10^{-6} M) solutions (a) and as thin films (b).

Electroluminescence and Electron Transport Properties. We investigated the intrinsic electroluminescence (EL) of the new polyquinolines by using poly(ethylenedioxythiophene)/poly(styrenesulfonic acid) (PEDOT) thin film on indium tin oxide (ITO) as the anode, poly(*N*-vinylcarbazole) (PVK) as the hole transport layer, the spin-coated polyquinoline as the emissive layer, and aluminum as the cathode: ITO/PEDOT/PVK/polyquinoline/Al. The film thicknesses of the emissive polyquinolines were ~ 75 nm. Representative EL spectra of four of the polymers are shown in Figure 6a. Emission maxima ($\lambda_{\text{max}}^{\text{EL}}$) varied from 513 to 656 nm (Table 3), indicating that we can effectively tune the emission color from blue-green to red by varying the arylene linkage. The EL maxima for PPOQ, PBOQ, and PSHQ are between 513 and 580 nm. The EL spectra for these polymers are considerably red-shifted 36–87 nm, relative to the PL spectra. The 551–656 nm EL maxima of PBTOQ, PBTVOQ, and PPZOQ are more consistent with the PL maxima.

The voltage–current and voltage–luminance curves for all six polyquinoline OLEDs are shown in Figure 7. The turn-on voltage (electric field) of the diodes was 8.5–12 V ($\sim 1.2 \times 10^6$ V/cm). PPZOQ, which has the smallest barrier to hole injection ($\text{IP} = 5.17$ eV), has the lowest turn-on voltage. The generally high turn-on voltages of these diodes are because of the large film thicknesses and the large barriers for charge injection.

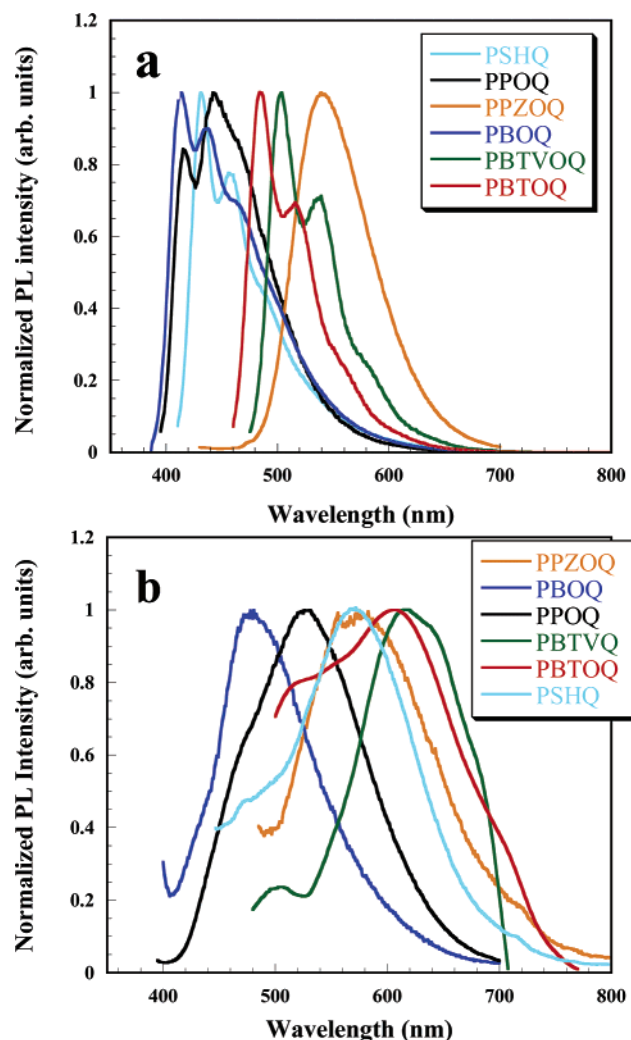


Figure 5. Photoluminescence (PL) spectra of new polyquinolines in dilute THF (10^{-6} M) solutions (a) and as thin films (b). All polymers were excited at their respective absorption maximum.

The brightness of the OLEDs was 69–209 cd/m^2 , and the external quantum efficiency (EQE) was 0.01–0.05% (Table 3). The device efficiency and brightness are in accord with the poor fluorescence quantum yields of thin films and the large barrier to hole injection into the *n*-type polymers. The OLED performance of the new polyquinolines is comparable to those of previous polyquinoline devices.^{6c,d,7,10,22}

n-Type (electron transport) polymers that can be used in bilayer OLED architectures with organic-solvent soluble emissive polymers are relatively scarce, although some polypyridines, polyquinolines, and polyquinoxalines that are soluble in formic acid have been explored.^{3a,6,7} Such an electron transport material (ETM) can increase device performance by reducing the barrier to electron injection, by blocking holes, and by moving the recombination zone away from the cathode. We have investigated the electron transport properties of the new polyquinolines by using MEH–PPV as the emissive polymer in LEDs of the type ITO/PEDOT/MEH–PPV/polyquinoline/Al. The film thickness of the polyquinolines as an electron transport layer in these diodes was in the range of 55–60 nm. These OLEDs showed EL spectra characteristic of MEH–PPV, having an emission peak at about 580 nm as exemplified in Figure 6b. The diodes showed no emission from the polyquinoline layer,

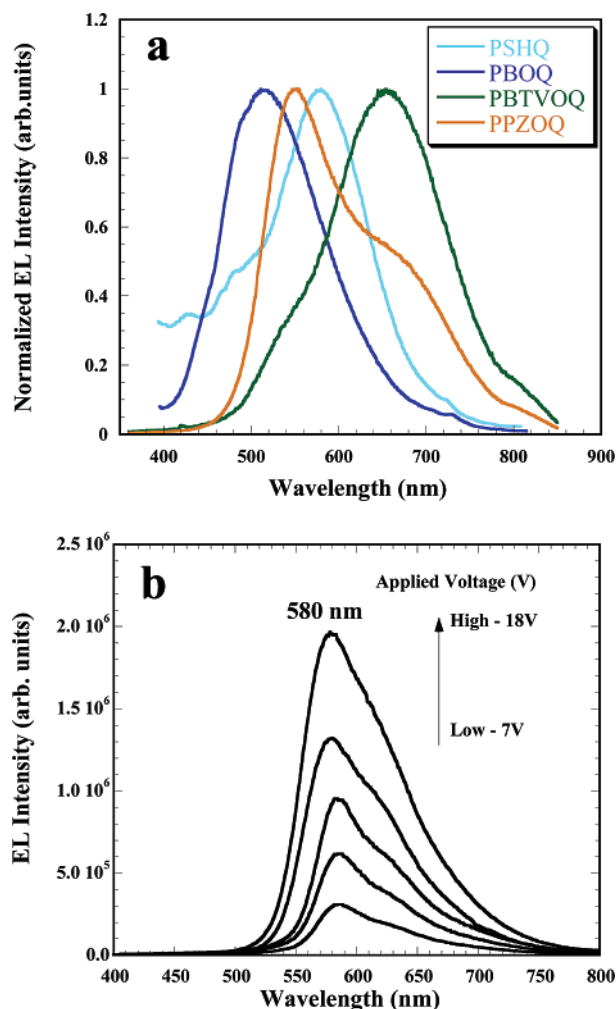


Figure 6. Electroluminescence (EL) spectra of selected polyquinolines in ITO/PEDOT/PVK/polyquinoline/Al diodes (a) and for a ITO/PEDOT/MEH-PPV/PPOQ/Al diode (b).

indicating that recombination was occurring strictly in the MEH-PPV. The current-voltage and luminance-voltage characteristics of the MEH-PPV diodes using the new polyquinolines as electron transport materials are shown in Figure 8. The turn-on voltage (electric field) of these LEDs was 4.5–8.0 V ($\sim 9 \times 10^5$ V/cm). The best performance was found in diodes using PBTVOQ as the electron transport material, achieving a brightness of 740 cd/m² and an external quantum efficiency of 0.12%. PSHQ based diodes had a similar brightness (659 cd/m²) and efficiency (0.11%) but a lower turn-on voltage of 4.5 V. This represents an increase in both brightness and efficiency over single-layer MEH-PPV devices or single-layer polyquinoline diodes. Diodes using the other polyquinolines as ETMs had bright-

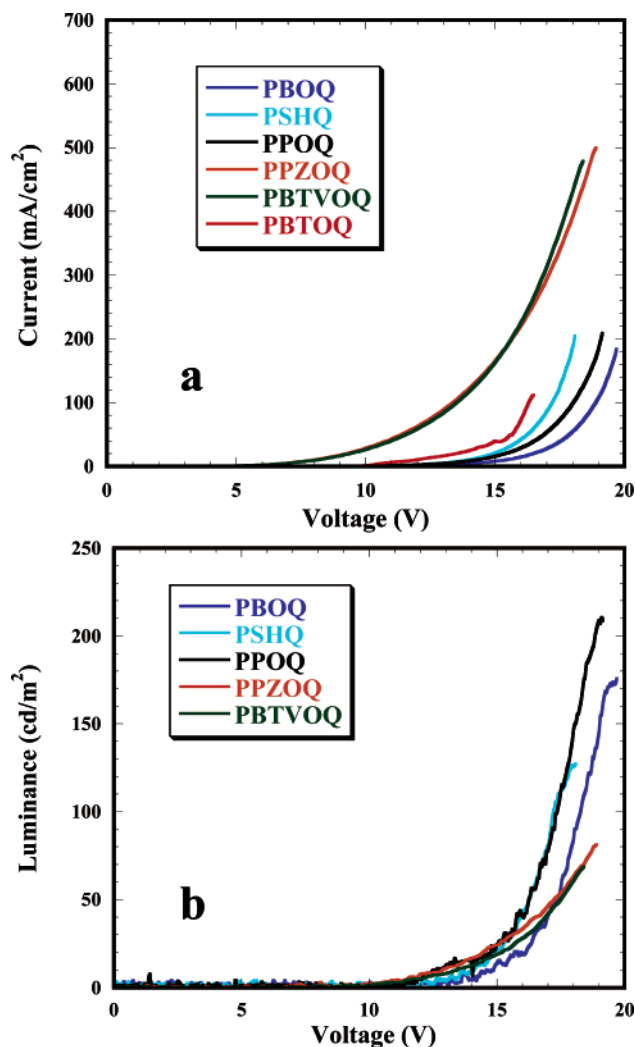


Figure 7. Current density-voltage characteristics (a) and luminance-voltage characteristics (b) for ITO/PEDOT/PVK/polyquinoline/Al diodes.

nesses of 451–557 cd/m² and EL device efficiencies (EQEs) between 0.08 and 0.11%. It is reasonable to conclude that the performance of all the MEH-PPV diodes incorporating these polyquinolines as ETMs is in the same range. The performance of these diodes is equal to or higher than other recent work where polyquinolines were employed strictly as the electron transport layer with emissive MEH-PPV.^{6e,f} However, these results are considerably lower than those based on polyquinolines incorporating a bis(phenylquinoline) and a regioregular dialkylbithiophene in the backbone.^{6c,d} The molecular weights of those previous polyquinolines were significantly higher ($(1.9\text{--}14.9) \times 10^4$) than the present materials.^{6c,d} The lower molecular weights of the

Table 3. Electroluminescent Device Properties of New Polyquinolines

polymer	as an emissive material ^a					as an electron transport material ^b				
	L_{max} (cd/m ²)	$\lambda_{\text{max}}^{\text{EL}}$ (nm)	J_{max} (mA/cm ²)	V_{on} (V)	EQE (%)	L_{max} (cd/m ²)	$\lambda_{\text{max}}^{\text{EL}}$ (nm)	J_{max} (mA/cm ²)	V_{on} (V)	EQE (%)
PPOQ	209	580	208	11	0.05	451	580	500	7.5	0.09
PBOQ	176	513	184	12	0.04	557	580	500	8	0.08
PSHQ	127	578	205	11	0.03	659	585	500	4.5	0.11
PBTOQ	25	610	110	9.5	0.005	n.o.	n.o.	n.o.	n.o.	n.o.
PBTVOQ	69	656	479	9	0.01	740	578	500	7.5	0.12
PPZOQ	81	551	500	8.5	0.02	470	575	496	7	0.08

^a Polyquinolines were in diodes of the type ITO/PEDOT/PVK/polyquinoline/Al. ^b The polyquinolines were in diodes of the type ITO/PEDOT/MEH-PPV/polyquinoline/Al.

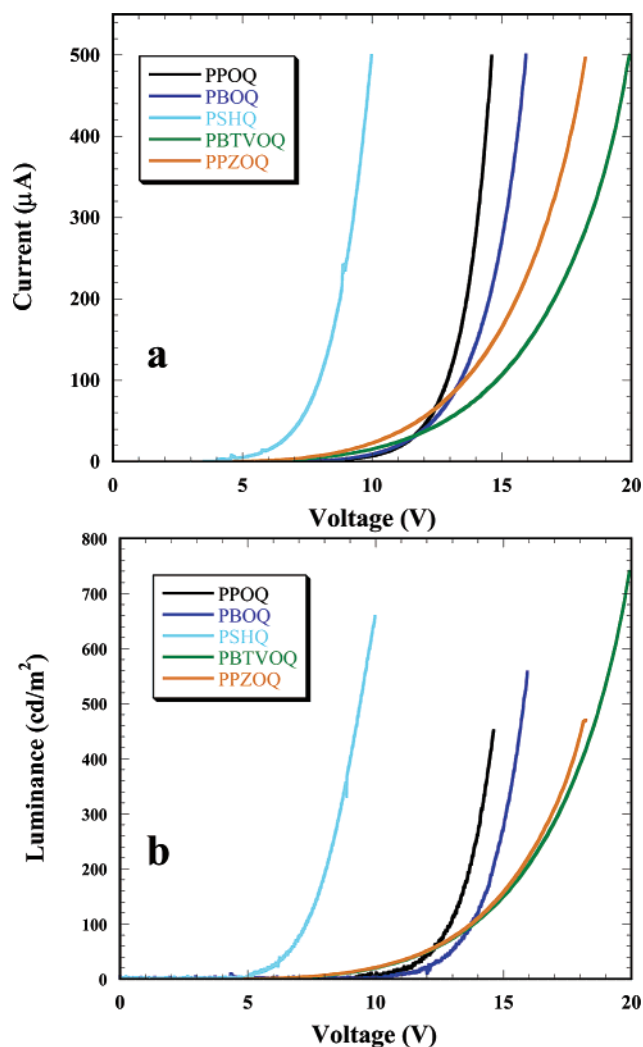


Figure 8. Current density–voltage characteristics (a) and luminance–voltage characteristics (b) for ITO/PEDOT/MEH–PPV/polyquinoline/Al diodes.

present polyquinolines may account for their poorer performance as ETMs, compared to our previously reported materials, since the electron affinities of the two classes of polyquinolines are comparable.

Conclusions

We have devised a new synthetic route to soluble *n*-type conjugated polyquinolines. Synthesis of the key *o*-amino keto-functionalized monomer, 3,3'-dinonanoylbenzidine (**5**), was achieved by reacting alkylmagnesium bromide with the appropriate carboxylic acid. The new polymers derived from this monomer contained bis(4-alkylquinoline) in the main chain, facilitating solubility in organic solvents. The polymers had glass transitions of 110–254 °C and decomposed at above 400 °C, proving them to be thermally robust materials suitable for application in organic electronic devices. By varying the arylene linkage in poly(2,2'-arylene-6,6'-bis(4-alkylquinoline)s from *p*-phenylene to bis(thienyl)vinylene, the optical band gap, redox properties, and electroluminescence color could be tuned over a wide range. The electron affinity or LUMO energy level of the polymers was in the range 2.72–3.00 eV, and blue-green, green, yellow, orange, and red electroluminescence colors were achieved with moderate brightness and efficiency. Enhanced electroluminescence efficiency and brightness

were obtained from bilayer OLEDs based on MEH–PPV as the emitter and the new polyquinolines as the electron transport layer.

The bis(4-alkylquinoline) platform demonstrated here allows the ready synthesis of diverse new soluble polyquinolines; it thus opens the door to further exploration of this *n*-type building block in new materials for organic electronics. New polymer structures incorporating more exotic arylene linkages may allow the optimization of the materials for improved performance in optoelectronic devices. Furthermore, optimization of the reaction conditions should lead to higher molecular weight polymers and could likely increase device performance.

Experimental Section

Materials. Diacetylbenzene, diacetyl biphenyl, 5-bromoanthranilic acid (**1**), 1-bromooctane, hexamethylditin, diphenyl phosphate (DPP), *m*-cresol, and Pd(PPh₃)₄ were purchased from Aldrich and were used as received with the exception of *m*-cresol, which was distilled prior to polymerization.

Synthetic Procedures. *N*-Trifluoroacetyl-5-bromoanthranilic acid (**2**),²³ 4,4'-diacetylstilbene,²⁴ 1,2-bis(5-acetyl-2-thienyl)ethylene,^{11b} 10-decylphenothiazine,²⁵ and 3,3'-heptanoylbenzidine (**8**)¹⁰ were synthesized according to literature procedures.

***N*-(Trifluoroacetyl)-5-bromo-3-nonanoylaniline (**3**).** 5 equiv of an ethereal solution of the octylmagnesium bromide was added to 11 g (35.0 mmol) of **2** in 500 mL of anhydrous THF at 0 °C. The reaction was refluxed overnight and then poured into water/CH₂Cl₂ mixture. The organic layer was separated and concentrated, washed with 1 M NaOH and water, and dried with MgSO₄, and the solvent was removed to yield an orange oil. The oil was purified on silica gel column (2:1 hexanes:CH₂Cl₂) to yield 9.3 g of pale orange oil (56%). ¹H NMR (499 MHz, CDCl₃, 298 K) δ (ppm): 12.89 (s, 1H); 8.67 (s, 1H); 8.14 (d, 1H); 7.74 (d, 1H); 3.05 (d, 2H); 1.75 (t, 2H); 1.35 (m, 6H); 0.92 (t, 3H).

***N,N*-(Trifluoroacetyl)-3,3'-dinonanoylbenzidine (**4**).** 13.9 g (35.3 mmol) of **3**, 6.0 g (18.3 mmol) of [Me₃Sn]₂, and 0.62 g (0.54 mmol) of Pd(PPh₃)₄ in 200 mL of anhydrous toluene were refluxed overnight. The reaction mixture was poured into CH₂Cl₂, and the resulting crystals were collected, dissolved in CH₂Cl₂, washed with H₂O several times, and dried, and the solvent was evaporated to yield an orange solid which was recrystallized from a mixture of CH₂Cl₂/MeOH to yield 6.0 g of orange needles (56%). ¹H NMR (499 MHz, CDCl₃, 298 K) δ (ppm): 12.89 (s, 2H); 8.76 (s, 2H); 8.07 (d, 2H); 7.75 (d, 2H); 3.05 (d, 4H); 1.75 (t, 4H); 1.35 (m, 12H); 0.92 (t, 6H). Calcd for C₃₀H₃₄F₆N₂O₄: C, 62.19; H, 6.45; F, 17.36; N, 4.27; O, 9.75. Found: C, 62.32; H, 6.10; N, 4.33.

3,3'-Dinonanoylbenzidine (5**).** 3.0 g (4.9 mmol) of **4** and 6.0 g (56.6 mmol) of Na₂CO₃ were added to a deaerated solution of 30 mL of H₂O and 100 mL of EtOH. The reaction mixture was refluxed for 3 days, poured into water/CH₂Cl₂ mixture, washed with water, and dried with MgSO₄, and the solvent was removed to yield 1.9 g of yellow needles (88%). ¹H NMR (499 MHz, CDCl₃, 298 K) δ (ppm): 7.88 (s, 2H); 7.47 (d, 2H); 6.75 (d, 2H); 6.32 (s, 4H); 3.02 (d, 4H); 1.79 (t, 4H); 1.35 (m, 12H); 0.93 (t, 6H). FT-IR (NaCl, cm⁻¹): 3435, 3323, 2920, 2852, 1651, 1624, 1552, 1481, 1258, 1179, 968, 820. Calcd for C₂₆H₃₆N₂O₄: C, 77.54; H, 9.54; N, 6.03; O, 6.89. Found: C, 77.57; H, 9.29; N, 6.07.

2,7-Diacetyl-10-decylphenothiazine (7**).** 10.5 g (80.0 mmol) of AlCl₃ was slowly added to a mixture of 12.3 g (36.2 mmol) of 10-decylphenothiazine (**6**) and 6.5 g (82.0 mmol) of acetyl chloride in CS₂ at 0 °C. The reaction was stirred at room temperature for 3 h and then poured into ice. The product was extracted into CH₂Cl₂ (3 × 100 mL) and then eluted through silica gel column with CH₂Cl₂. The yellow solid was recrystallized twice from hexanes to yield 5.3 g (39%) of yellow needles. FT-IR (NaCl, cm⁻¹): 2917, 2849, 1670, 1565, 1476, 1355, 1266, 1238, 796. ¹H NMR (499 MHz, CDCl₃, 298 K) δ (ppm): 7.70 (m, 4H); 6.90 (d, 2H); 3.92 (t, 2H); 2.55 (s, 6H); 2.49 (m, 2H),

1.83 (m, 2H), 1.27 (m, 14H), 0.91 (d, 3H). Calcd for $C_{22}H_{29}NS$: C, 77.82; H, 8.61; N, 4.13; S, 9.44. Found: C, 77.53; H, 8.51; N, 3.77.

General Procedure for Polymerization. 1 equiv of the diacetyl monomer, 1 equiv of 3,3'-dinonanoylbenzidine, 6.0 g of diphenyl phosphate, and 3 g of *m*-cresol were added to a cylindrical reaction vessel. The reactor was purged with argon for 20 min. The mixture was mechanically stirred under static argon as the temperature was gradually raised to 140 °C over a period of 12 h. The polymerization mixture was stirred at this temperature for 72 h and then precipitated into 10% triethylamine/ethanol. The precipitate was collected by vacuum filtration and extracted on a Soxhlet apparatus for 72 h with 20% triethylamine/ethanol. The polymer was dissolved in $CHCl_3$ and precipitated into ethanol, collected by vacuum filtration, and dried at 60 °C in a vacuum for 24 h.

Poly(2,2'-(*p*-phenylene)-6,6'-bis(4-octylquinoline)) (PPOQ). 570 mg of yellow solid recovered (90% yield). 1H NMR (499 MHz, $CDCl_3$, 298 K) δ (ppm): 8.18 (d, 2H); 8.09 (s, 2H); 7.99 (d, 2H); 7.77 (s, 2H); 7.61 (d, 2H); 7.54 (d, 2H); 2.60 (s, 4H); 1.70 (m, 4H); 1.35 (m, 20H); 0.77 (t, 6H). FT-IR (NaCl, cm^{-1}): 3059, 2924, 2853, 1593, 1553, 1495, 1347, 1298, 1240, 1107, 1015, 826, 754.

Poly(2,2'-(4,4'-diphenylene)-6,6'-bis(4-octylquinoline)) (PBOQ). 585 mg of yellow solid recovered (85% yield). 1H NMR (499 MHz, $CDCl_3$, 298 K) δ (ppm): 8.22 (d, 2H); 8.11 (s, 2H); 8.01 (d, 2H); 7.78 (s, 2H); 7.71 (d, 4H); 7.60 (d, 4H); 2.67 (s, 4H); 1.66 (m, 4H); 1.28 (m, 20H); 0.85 (t, 6H). FT-IR (NaCl, cm^{-1}): 3032, 2924, 2853, 1593, 1495, 1354, 1005, 825.

Poly(2,2'-(4,4'-stilbene)-6,6'-bis(4-hexylquinoline)) (PSHQ). 3,3'-Diheptanoylbenzidine was used in place of 3,3'-dinonanoylbenzidine. 0.450 g (87%) of pale yellow powder was recovered. 1H NMR (499 MHz, $CDCl_3$, 298 K) δ (ppm): 8.21 (d, 2H); 8.11 (s, 2H); 8.01 (d, 2H); 7.66 (s, 2H); 7.55 (d, 4H); 7.43 (d, 4H); 3.75 (dd, 2H); 2.68 (s, 4H); 1.68 (m, 4H); 1.28 (m, 12H); 0.85 (t, 6H).

Poly(2,2'-(5-(2-thien-2-ylethenyl)thien-2-yl)-6,6'-bis(4-hexylquinoline)) (PBTOQ). 330 mg of orange solid recovered (51% yield). 1H NMR (499 MHz, $CDCl_3$, 298 K) δ (ppm): 8.35 (d, 2H); 8.17 (s, 2H); 8.06 (d, 2H); 7.54 (s, 2H); 7.05 (d, 4H); 6.93 (d, 4H); 2.67 (s, 4H); 1.66 (m, 4H); 1.28 (m, 20H); 0.91 (t, 6H). FT-IR (cm^{-1}): 2924, 2854, 1653, 1558, 1541, 1457, 1357, 1227, 1194, 1041, 926, 852, 721, 667.

Poly(2,2'-(5-(2-thien-2-ylethenyl)thien-2-yl)-6,6'-bis(4-hexylquinoline)) (PBTVOQ). 370 mg of orange solid recovered (86% yield). 1H NMR (499 MHz, $CDCl_3$, 298 K) δ (ppm): 8.35 (d, 2H); 8.17 (s, 2H); 8.06 (d, 2H); 7.54 (s, 2H); 7.05 (d, 4H); 6.93 (d, 4H); 3.33 (dd, 2H); 2.67 (s, 4H); 1.66 (m, 4H); 1.28 (m, 20H); 0.91 (t, 6H). FT-IR (cm^{-1}): 2920, 2902, 1585, 1544, 1456, 1421, 1022, 826, 699, 621.

Poly(2,2'-(10-decylphenothiazine-2,7-diyl)-6,6'-bis(4-octylquinoline)) (PPZOQ). 470 mg of orange solid recovered (75% yield). 1H NMR (499 MHz, $CDCl_3$, 298 K) δ (ppm): 8.31 (d, 2H); 8.27 (s, 2H); 8.03 (d, 2H); 7.77 (s, 2H); 7.61 (d, 2H); 7.31 (d, 2H); 7.03 (s, 2H); 3.65 (d, 2H); 2.68 (s, 4H); 1.83 (m, 2H); 1.28 (m, 38H); 1.05 (t, 3H) 0.88 (t, 6H). FT-IR (NaCl, cm^{-1}): 3059, 2924, 2853, 1593, 1495, 1466, 1347, 1015, 841.

General. 1H NMR spectra were recorded on a Bruker DRX-499 at 499 MHz using $CDCl_3$ as the solvent. Fourier transformation infrared (FT-IR) spectroscopy was done on a film on a NaCl plate using a Perkin-Elmer 1720 FT-IT spectrometer. Thermogravimetric analysis of the polymers was conducted on a TA Instruments Q50 TGA. A heating rate of 10 °C/min under flowing N_2 was used with runs being conducted from room temperature to 800 °C. Differential scanning calorimetry (DSC) was run on a TA Instruments Q100 DSC under flow of N_2 . The heat-cool-heat method was used with an initial heat rate of 20 °C/min and a cooling rate of 10 °C/min and a final heating rate of 10 °C/min. All reported transitions were based upon the second heating.

Photophysics. Optical absorption spectra were obtained by using a Lambda-900 UV/vis/near-IR spectrophotometer (Perkin-Elmer). Steady-state photoluminescence (PL) studies were done by using a Photon Technology International Inc. (PTI) instrument and a Xe lamp (75 W) as the excitation source

in air at room temperature. In solution, the fluorescence quantum yield in 10^{-6} M THF was determined using a perylene standard (87%). A rough estimate of the fluorescence quantum yield in the solid state was achieved by comparing the thin film of the polymer with a thin film of 9,10-diphenylanthracene in poly(methyl methacrylate) as a reference standard (83%).²⁶

Cyclic Voltammetry. Cyclic voltammetry experiments were done on an EG&G Princeton Applied Research potentiostat/galvanostat (model 273A). Data were collected and analyzed by the model 270 Electrochemical Analysis System Software on a PC computer. A three-electrode cell was used in all experiments as previously described.^{17,18} Platinum wire electrodes were used as both counter and working electrodes, and silver/silver ion (Ag in 0.1 M $AgNO_3$ solution, Bioanalytical System, Inc.) was used as a reference electrode. The Ag/Ag^+ ($AgNO_3$) reference electrode was calibrated at the beginning of the experiments by running cyclic voltammetry on ferrocene as the internal standard in an identical cell without any polymer on the working electrode. By means of the internal ferrocenium/ferrocene (Fc^+/Fc) standard, the potential values, obtained in reference to Ag/Ag^+ electrode, were converted to the saturated calomel electrode (SCE) scale. The films of all polymers were coated on the Pt working electrode by dipping the Pt wire into the viscous solution in chloroform and then drying it in a vacuum oven at 80 °C for 8 h. An electrolyte solution of 0.1 M TBAPF₆ in acetonitrile was used in all experiments. All solutions in the three-electrode cell were purged with ultrahigh-purity N_2 for 10–15 min before each experiment, and a blanket of N_2 above the solution was used during the experiment.

Fabrication and Characterization of LEDs. Two types of OLEDs were fabricated and evaluated: ITO/PEDOT/PVK/polyquinoline/Al and ITO/PEDOT/MEH-PPV/polyquinoline/Al. Sequential spin-coating of the layers onto a cleaned ITO-coated glass substrate was used to fabricate the devices. A thin layer of poly(ethylenedioxythiophene)-poly(styrenesulfonate) (PEDOT) (~40 nm) was first spin-coated from its solution in water onto ITO and dried at 80 °C in a vacuum for 12 h. For ITO/PEDOT/PVK/polyquinoline/Al devices, PVK thin film was spin-coated from a 0.5 wt % solution in $CHCl_3$ onto the PEDOT layer and dried at 50 °C in a vacuum for 10 h. In the case of ITO/PEDOT/MEH-PPV/polyquinoline/Al devices, the MEH-PPV thin film was spin-coated from a 0.5 wt % solution in $CHCl_3$ onto the PEDOT layer and dried at 50 °C in a vacuum for 10 h. A thin film of the polyquinoline was then spin-coated from a 0.5 wt % solution in formic acid onto the MEH-PPV thin film. The multilayer thin films were dried in a vacuum at 80 °C for 10 h before deposition of the aluminum electrode under vacuum (3×10^{-6} Torr). A 100 nm thick aluminum layer was thermally deposited to form active diode areas of 0.2 cm² (5 mm diameter).

The film thickness was measured by using an Alpha step profilometer (model 500, KLA-Tencor, San Jose, CA), which has a resolution of ± 1 nm. Electroluminescence (EL) spectra were measured on a Photon Technology International Inc. (PTI) Instrument fluorimeter. The electrical characteristics of the devices were measured on an HP4155A semiconductor parameter analyzer together with a Grasby S370 optometer equipped with a calibrated luminance sensor head. The EL quantum efficiencies of the diodes were measured by using the procedures similar to those previously reported.²⁷ All the fabrications and measurements were done under ambient laboratory conditions.

Acknowledgment. C.T. thanks Angela P. Gifford for her assistance in purifying new materials and Dr. XiangXing Kong for supplying the *N*-decylphenothiazine. This research was supported by the NSF STC-MDITR at the University of Washington, the NSF (CTS-0437912), and in part by the Air Force Office of Scientific Research (Grant F49620-03-1-0162).

References and Notes

- (1) See the special issue on organic electronics: Jenekhe, S. A. *Chem. Mater.* **2004**, *16*, 4381.
- (2) (a) Kelley, T. W.; Baude, P. F.; Gerlach, C.; Ender, D. E.; Muyres, D.; Haase, M. A.; Vogel, D. E.; Theiss, S. D. *Chem. Mater.* **2004**, *16*, 4413. (b) Newman, C. R.; Frisbie, C. D.; da Silva Filho, D. A.; Bredas, J. L.; Ewbank, P. C.; Mann, K. R. *Chem. Mater.* **2004**, *16*, 4436. (c) Dimitrakopoulos, C. D.; Malenfant, P. R. L. *Adv. Mater.* **2002**, *14*, 99. (d) Babel, A.; Jenekhe, S. A. *Adv. Mater.* **2002**, *14*, 371. (e) Babel, A.; Jenekhe, S. A. *J. Am. Chem. Soc.* **2003**, *125*, 13656. (f) Chua, L.-L.; Zaumseil, J.; Chang, J.-F.; Ou, E. C.-W.; Ho, P. K.-H.; Sirringhaus, H.; Friend, R. H. *Nature (London)* **2005**, *434*, 194. (g) Yamamoto, T.; Kokubo, H.; Kobashi, M.; Sakai, Y. *Chem. Mater.* **2004**, *16*, 4616.
- (3) Reviews on organic electroluminescence: (a) Kraft, A.; Grimsdale, A. C.; Holmes, A. B. *Angew. Chem., Int. Ed.* **1998**, *37*, 402. (b) Heeger, A. J. *Solid State Commun.* **1998**, *107*, 673. (c) Bernius, M. T.; Inbasekaran, M.; O'Brien, J.; Wu, W. *Adv. Mater.* **2000**, *12*, 1737. (d) Kulkarni, A. P.; Tonzola, C. J.; Babel, A.; Jenekhe, S. A. *Chem. Mater.* **2004**, *16*, 4556.
- (4) (a) Coakley, K. M.; McGehee, M. D. *Chem. Mater.* **2004**, *16*, 4533. (b) Alam, M. M.; Jenekhe, S. A. *Chem. Mater.* **2004**, *16*, 4647. (c) Jenekhe, S. A.; Yi, S. *Appl. Phys. Lett.* **2000**, *77*, 2635.
- (5) (a) Marsitzky, D.; Scott, J. C.; Chen, J.-P.; Lee, V. Y.; Miller, R. D.; Setayesh, S.; Mullen, K. *Adv. Mater.* **2001**, *13*, 1096. (b) Liao, L.; Pang, Y.; Ding, L.; Karasz, F. E. *Macromolecules* **2004**, *37*, 3970. (c) Tarkka, R. M.; Zhang, X.; Jenekhe, S. A. *J. Am. Chem. Soc.* **1996**, *118*, 9438.
- (6) (a) Jenekhe, S. A.; Zhang, X.; Chen, X. L.; Choong, V.-E.; Gao, Y.; Hsieh, B. R. *Chem. Mater.* **1997**, *9*, 409. (b) Zhang, X.; Jenekhe, S. A. *Macromolecules* **2000**, *33*, 2069. (c) Tonzola, C. J.; Alam, M. M.; Jenekhe, S. A. *Adv. Mater.* **2002**, *14*, 1086. (d) Tonzola, C. J.; Alam, M. M.; Bean, B. A.; Jenekhe, S. A. *Macromolecules* **2004**, *37*, 3554. (e) Kim, J. L.; Kim, J. K.; Cho, H. N.; Kim, D. Y.; Kim, C. Y.; Hong, S. I. *Synth. Met.* **2000**, *114*, 97. (f) Kim, D. Y.; Lee, S. K.; Kim, J. L.; Kim, J. K.; Lee, H.; Cho, H. N.; Hong, S. I.; Kim, C. Y. *Synth. Met.* **2001**, *121*, 1707.
- (7) (a) Zhu, Y.; Alam, M. M.; Jenekhe, S. A. *Macromolecules* **2002**, *35*, 9844. (b) Zhu, Y.; Alam, M. M.; Jenekhe, S. A. *Macromolecules* **2003**, *36*, 8958.
- (8) (a) Krüger, H.; Janietz, S.; Sainova, D.; Wedel, A. *Macromol. Chem. Phys.* **2003**, *204*, 1607. (b) Kim, J. L.; Kim, J. K.; Cho, H. N.; Kim, D. Y.; Kim, C. Y.; Hong, S. I. *Macromolecules* **2000**, *33*, 5880.
- (9) (a) Chen, C.-H.; Shu, C.-F. *J. Polym. Sci., Part A: Polym. Chem.* **2004**, *42*, 3314. (b) Zhan, X.; Liu, Y.; Wu, X.; Wang, S.; Zhu, D. *Macromolecules* **2002**, *35*, 2529.
- (10) Tonzola, C. J.; Alam, M. M.; Jenekhe, S. A. *Macromol. Chem. Phys.* **2005**, *206*, 1271.
- (11) (a) Agrawal, A. K.; Jenekhe, S. A. *Chem. Mater.* **1992**, *4*, 95. (b) Agrawal, A. K.; Jenekhe, S. A. *Macromolecules* **1993**, *26*, 895. (c) Agrawal, A. K.; Jenekhe, S. A. *Chem. Mater.* **1993**, *5*, 633.
- (12) (a) Alam, M. M.; Tonzola, C. J.; Jenekhe, S. A. *Macromolecules* **2003**, *36*, 6577. (b) Hide, F.; Yang, C. Y.; Heeger, A. J. *Synth. Met.* **1997**, *85*, 1355.
- (13) (a) Virgili, T.; Lidzey, D. G.; Bradley, D. D. C. *Adv. Mater.* **2000**, *12*, 58. (b) Gong, X.; Robinson, M. R.; Ostrowski, J. C.; Moses, D.; Bazan, G. C.; Heeger, A. J. *Adv. Mater.* **2002**, *14*, 581.
- (14) (a) Jenekhe, S. A.; Chen, X. L. *Science* **1998**, *279*, 1903. (b) Jenekhe, S. A.; Chen, X. L. *Science* **1999**, *283*, 372. (c) Chen, X. L.; Jenekhe, S. A. *Macromolecules* **2000**, *33*, 4610.
- (15) (a) Lu, L.; Jenekhe, S. A. *Macromolecules* **2001**, *34*, 6249. (b) Economopoulos, S. P.; Andreopoulos, A. K.; Gregoriou, V. G.; Kallitsis, J. K. *Chem. Mater.* **2005**, *17*, 1063.
- (16) Chiang, C.-L.; Shu, C.-F. *Chem. Mater.* **2002**, *14*, 682.
- (17) Agrawal, A. K.; Jenekhe, S. A. *Chem. Mater.* **1996**, *8*, 579.
- (18) (a) Yang, C. J.; Jenekhe, S. A. *Macromolecules* **1995**, *28*, 1180. (b) Alam, M. M.; Jenekhe, S. A. *J. Phys. Chem. B* **2002**, *106*, 11172.
- (19) (a) Jenekhe, S. A.; Lu, L.; Alam, M. M. *Macromolecules* **2001**, *34*, 7315. (b) Zhu, Y.; Yen, C. T.; Jenekhe, S. A.; Chen, W. C. *Macromol. Rapid Commun.* **2004**, *25*, 1829.
- (20) Yamamoto, T.; Zhou, Z.; Kanbara, T.; Shimura, M.; Kizu, K.; Maruyama, T.; Nakamura, Y.; Fukuda, T.; Lee, B.-L.; Ooba, N.; Tomaru, S.; Kurihara, T.; Kaino, T.; Kubota, K.; Sasaki, S. *J. Am. Chem. Soc.* **1996**, *118*, 10389.
- (21) (a) Jenekhe, S. A.; Osaheni, J. A. *Science* **1994**, *265*, 765. (b) Osaheni, J. A.; Jenekhe, S. A. *Macromolecules* **1994**, *27*, 739.
- (22) (a) Zhang, X.; Shetty, A. S.; Jenekhe, S. A. *Acta Polym.* **1997**, *49*, 52. (b) Zhang, X.; Shetty, A. S.; Jenekhe, S. A. *Macromolecules* **1999**, *32*, 7422. (c) Kwon, T. W.; Alam, M. M.; Jenekhe, S. A. *Chem. Mater.* **2004**, *16*, 4657.
- (23) Zhang, P.; Terefenko, E. A.; Slavin, J. *Tetrahedron Lett.* **2001**, *42*, 2097.
- (24) Zimmermann, E. K.; Stille, J. K. *Macromolecules* **1985**, *18*, 321.
- (25) Gilman, H.; Shirley, D. A. *J. Am. Chem. Soc.* **1944**, *66*, 888.
- (26) Heinrich, G.; Schoof, S.; Gusten, H. *J. Photochem.* **1974**, *3*, 315.
- (27) (a) Kulkarni, A. P.; Jenekhe, S. A. *Macromolecules* **2003**, *36*, 5285. (b) Okamoto, S.; Tanaka, K.; Izumi, Y.; Adachi, H.; Yamaji, T.; Suzuki, T. *Jpn. J. Appl. Phys.* **2001**, *40*, L783. (c) Kulkarni, A. P.; Kong, X.; Jenekhe, S. A. *J. Phys. Chem. B* **2004**, *108*, 8689.

MA051280B